Nano World Journal

https://doi.org/10.17756/nwj.2025-147

Research Article

Open Access

# α-Formamidinium Lead Iodide Perovskite Embedded in a Polyvinylidene Fluoride Matrix for Light-assisted Energy Harvesting and Sensing Applications

**Niloy Mridha, Chandra Mouli Nannapaneni, Shewli Pratihar, Aswani Yella and Prasanna Kumar S Mural***

*Department of Metallurgical Engineering and Materials Science, Indian Institute of Technology Bombay, Mumbai, India*

***Correspondence to:**
Prasanna Kumar S Mural
Department of Metallurgical Engineering and Materials Science,
Indian Institute of Technology Bombay,
Mumbai, India.
**E-mail:** prasannamural@iitb.ac.in

**Received:** December 11, 2025
**Accepted:** December 26, 2025
**Published:** December 31, 2025

**Citation:** Mridha N, Nannapaneni CM, Pratihar S, Yella A, Mural PKS. 2025. α-Formamidinium Lead Iodide Perovskite Embedded in a Polyvinylidene Fluoride Matrix for Light-assisted Energy Harvesting and Sensing Applications. *NanoWorld J* 11(4): 36-40.

Copyright: © 2025 Mridha et al. This is an Open Access article distributed under the terms of the Creative Commons Attribution 4.0 International License (CCBY) (http://creativecommons.org/licenses/by/4.0/) which permits commercial use, including reproduction, adaptation, and distribution of the article provided the original author and source are credited.

Published by United Scientific Group

## Abstract

Recent advances in energy harvesting have enabled efficient conversion of mechanical and light energy into electricity, with piezoelectric and photo-assisted hybrid strategies emerging as key drivers for flexible, high-performance, and eco-friendly self-powered systems. In this study, we demonstrate a straightforward strategy to stabilize α-formamidinium lead iodide (α-$FAPbI_3$) by embedding it within a polyvinylidene fluoride (PVDF) matrix, yielding a stable composite film as confirmed by X-ray diffraction (XRD) analysis. Composite films of α-$FAPbI_3$ and PVDF were prepared in varying ratios and systematically optimized by evaluating their ferroelectric behavior, including saturation polarization, remnant polarization, and energy storage density. Among these, 210 μL of α-$FAPbI_3$ in 1 g PVDF (FPF-3 composition) exhibited the most optimized performance. The photoactivity of the stabilized α-phase $FAPbI_3$, coupled with the intrinsic piezoelectric properties of PVDF, offers a synergistic platform for advanced photo-assisted energy harvesting applications. The photo-assisted energy harvesting device fabricated from the optimized composite exhibited distinct output variations under dark conditions, white light, and ultraviolet (UV) light exposure (360 nm and 390 nm), highlighting its potential for photo-assisted energy harvesting. Notably, a ~62.02% enhancement in output voltage was achieved under white light illumination. The optimized light-assisted device exhibited remarkable output enhancement, highlighting its potential as a promising candidate for next-generation self-powered energy systems.

## Keywords

α-Formamidinium lead iodide, Polyvinylidene fluoride, Piezoelectricity, Photo-assisted energy harvesting

## Introduction

Perovskite-PVDF composites have gained attention for their enhanced piezoelectric response and energy harvesting potential. $FAPbI_3$ absorbers possess narrower bandgaps and superior thermal stability among perovskites, enabling higher solar energy conversion efficiency and longer device lifetimes. However, despite these advantages, they suffer from phase instability during fabrication and operation [1]. The photoactive black α-phase of $FAPbI_3$ perovskite is metastable and typically forms at elevated temperatures above 150 °C. The cubic phase exhibits a higher formation enthalpy ($\Delta H_f$) than the hexagonal phase (δ), giving it a higher Gibbs free energy at 0 K. With increasing temperature, entropy from FA cation rotation lowers the Gibbs free energy of the cubic phase below that of the hexagonal phase. Upon cooling, the system reverts to the energetically favored hexagonal phase [2]. Recent studies verify that PVDF incorporation can enhance perovskite crystallinity, enlarge grain size, and improve optical absorption

by modulating crystal growth and interfacial properties, supporting its active role in improving polarization and interfacial charge transport in the present composite system [3]. Also, in some studies it is reported that, improvements in the performance of the perovskite were primarily achieved through Schottky junction optimization and PVDF-assisted enhancement of rectification, carrier concentration, and stability in perovskite systems [3, 4]. Building on these findings, the present work extends the Schottky framework to a PVDF/$FAPbI_3$ bulk composite, enabling distributed internal interfaces and polarization-induced fields that deliver enhanced energy harvesting performance and operational stability. In this study, we present a simple approach of solution-processed, spin-coated composite of α-$FAPbI_3$ embedded in PVDF. Within the composite, the perovskite exhibits a highly stable, non-reversible α-phase under ambient conditions. At the optimized α-$FAPbI_3$ loading FPF-3 composition, the composite exhibited a remarkable enhancement in the ferroelectric and piezoelectric properties of PVDF, as reflected in significantly improved saturation and remnant polarization values. Recent studies have shown that PVDF incorporation enhances carrier concentration and Schottky rectification in perovskite systems by improving crystallinity and interfacial interactions [3]. A photo-assisted energy harvesting device was fabricated to evaluate performance under different illumination conditions. Hand-tapping responses revealed output voltages of ~23.7 V (dark), ~38.4 V (white light), ~52.25 V (UV-390 nm), and ~62.6 V (UV-360 nm). Illumination enhanced the output by ~62.02%, demonstrating the device's strong potential for photo-assisted energy harvesting applications. In this context, the ~62.02% light-assisted voltage enhancement observed in the present work is attributed to photo-induced carrier modulation at the PVDF-perovskite interface, which strengthens Schottky barrier asymmetry and promotes efficient directional charge transport.

# Materials and Methods

## Materials

Formamidinium acetate (99%), hydroiodic acid (57 wt.% in water, distilled, stabilized, 99.95%), diethyl ether (97%), lead iodide (99%), N,N-dimethylformamide (anhydrous, 99.8%), and polyethylene terephthalate (PET)-based indium tin oxide (ITO) substrates were obtained from Sigma Aldrich. PVDF pellets Inoflar™ 1020 was procured from Gujarat Fluorochemicals Limited, ethanol (99.9%) from Changshu Hongsheng Fine Chemicals Ltd., and polydimethylsiloxane from Dow Chemicals. All chemicals were used as received without any further purification or modification.

## Methods

### $FAPbI_3$ synthesis

Formamidinium iodide (FAI) was synthesized by dissolving formamidinium acetate in a two-fold molar excess of 57 wt.% hydroiodic acid and stirring at 50 °C for 10 min. The product was dried at 100 °C to yield a white powder with a faint golden hue, washed with diethyl ether, and recrystallized twice from ethanol to obtain pure needle-like crystals. The final product was dried overnight in a vacuum oven. For the preparation of $FAPbI_3$ solution, FAI and lead(II) iodide were mixed in a 1:1 molar ratio in dimethylformamide (DMF) to obtain a 1 M solution.

### PVDF/$FAPbI_3$ composite preparation

The PVDF/$FAPbI_3$ composites were synthesized via spin coating and solvent evaporation, using PVDF dissolved in DMF followed by stirring at 50 °C to form a uniform solution before adding the perovskite. Different $FAPbI_3$-loaded PVDF composites (FPF-1: 70 µl/g, FPF-2: 140 µl/g, FPF-3: 210 µl/g, and FPF-4: 280 µl/g of PVDF) The resulting films were spin-coated at 1000 revolutions per minute (rpm) for 20 s and annealed at 150 °C to obtain the final composites.

### Light assisted energy harvesting device fabrication

The light-assisted piezoelectric nanogenerator was fabricated using a PET-based ITO substrate (2.5 × 3 cm). The substrate was centrally etched with zinc dust and 48% hydrochloride acid to form two electrodes, followed by sequential cleaning with soap solution, deionized water, acetone, and ethanol under sonication for 10 min. A 15 min UV-ozone treatment was then performed before depositing the PVDF/$FAPbI_3$ composite. The composite solution was spin-coated onto the substrate at 1000 rpm for 20 s and subsequently annealed at 150 °C to obtain the final device.

# Characterizations

## Wide angle XRD (WAXRD) analysis

WAXD measurements were performed on the films using a PANalytical X'Pert Pro diffractometer with Cu-Kα radiation (λ = 1.54 Å, 45 kV, 30 mA). Data were collected over a 2θ range of 10 - 60° with a step size of 0.02° and a dwell time of 30 s per step. The nanocomposite films analyzed had an area of 1 $cm^2$ and an approximate thickness of 1.5 mm.

## Ferroelectric property analysis

Ferroelectric polarization-electric field (P-E) loop measurements were carried out on pure PVDF and FPF composite films using a triangular waveform at 50 Hz and 1 Hz under varying voltages at room temperature with a TF analyzer 2000 (aixACCT, Germany).

# Results and Discussion

Figure 1a shows the XRD patterns of α-$FAPbI_3$ along with the corresponding crystal lattice structures. The α-phase is characterized by a cubic lattice. The XRD pattern of the α-phase displays distinct peaks at 13.9°, 19.8°, 24.3°, 28.1°, 31.4°, 34.6°, 40.1°, and 42.7° [5]. Figure 1b illustrates the XRD patterns of PVDF composite films embedded with α-$FAPbI_3$. The analysis confirms the stabilization of the α-$FAPbI_3$ phase upon composite formation with PVDF, achieved at annealing temperatures of 150 °C (black film). The XRD profiles reveal that the characteristic diffraction peaks of $FAPbI_3$ appear at identical positions to those observed in pristine $FAPbI_3$ apart from the PVDF peaks. In the present study, stabilization of the α-$FAPbI_3$ phase is achieved within the PVDF matrix because the polymer framework suppresses the rotational

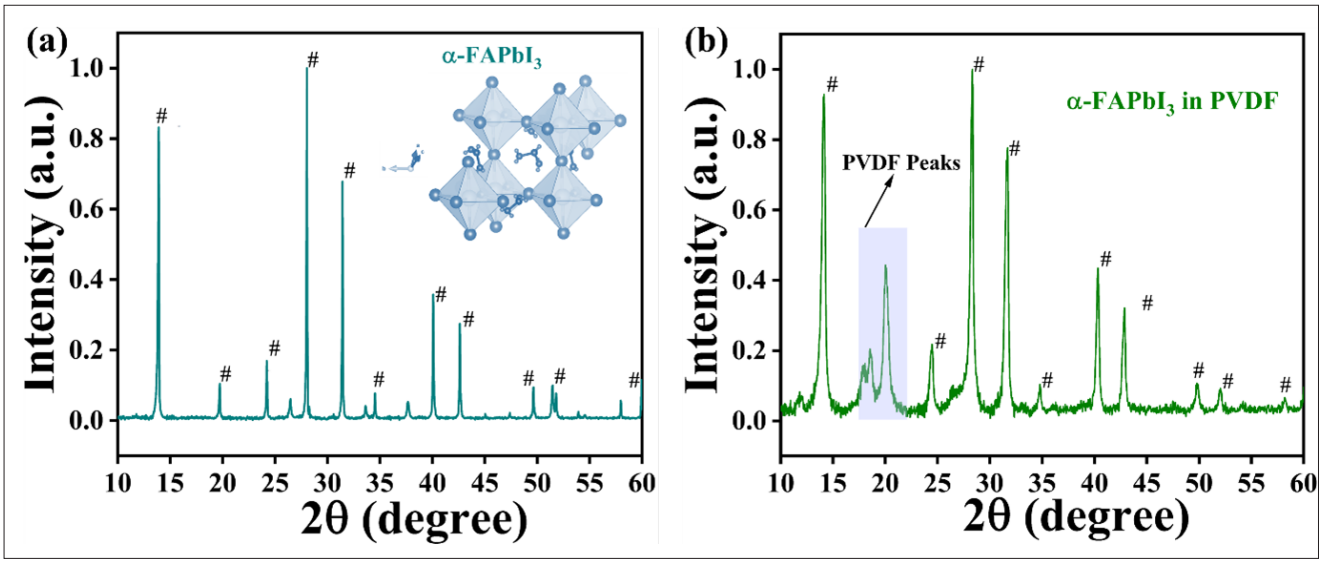



**Figure 1: (a)** XRD pattern of the α-$FAPbI_3$ and **(b)** XRD pattern of the PVDF/$FAPbI_3$ composite.

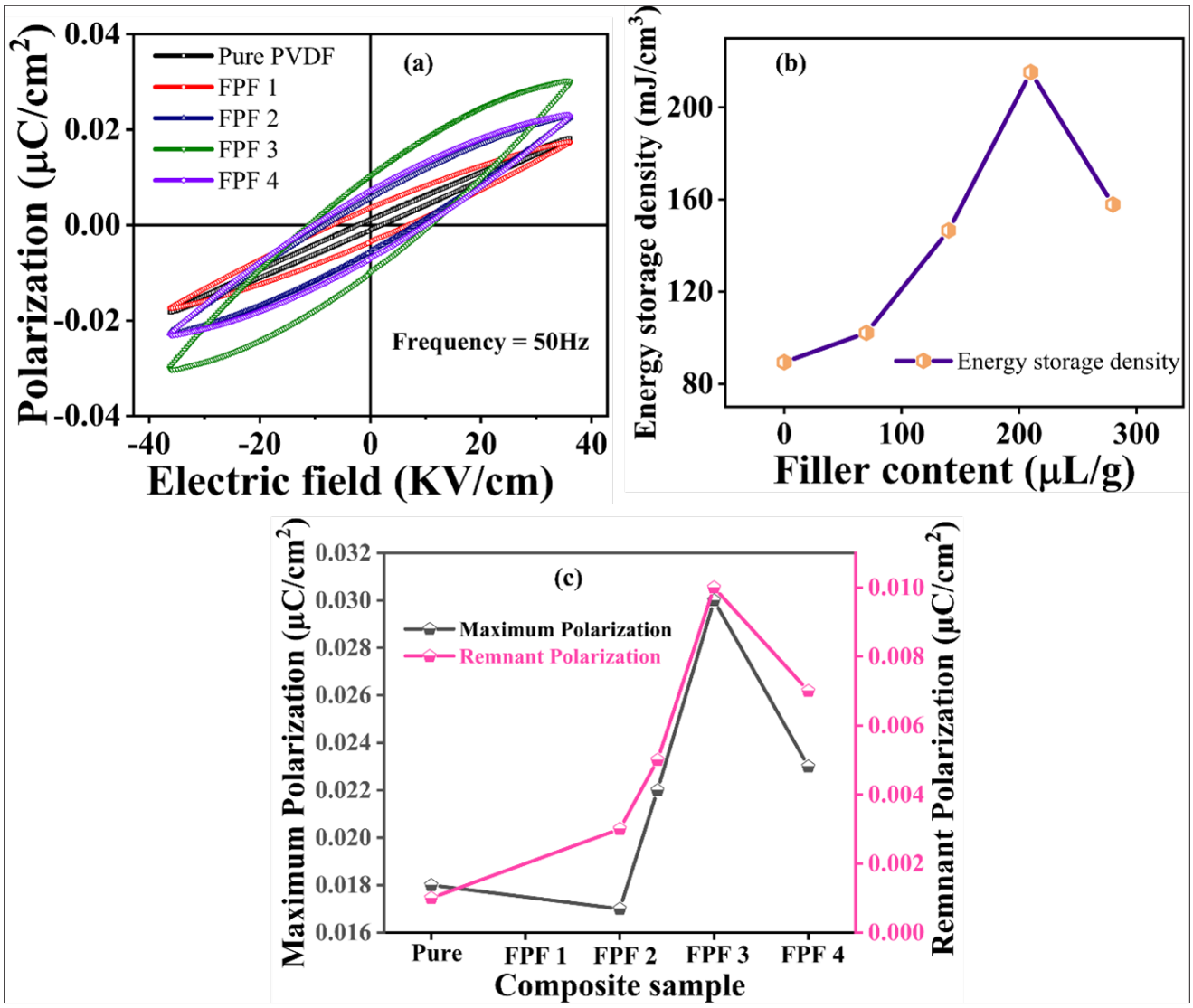



**Figure 2: (a)** Ferroelectric property, P-E loop of PVDF and FPF composites, **(b)** energy storage density achieved by different composites, and **(c)** maximum saturation polarization and remnant polarization achieved by different composites.

disorder of FA cations through strong interfacial confinement and electrostatic interactions, thereby facilitating the retention of the α-phase at room temperature [6].

Figure 2a presents the ferroelectric P-E loops of PVDF and PVDF/$FAPbI_3$ composites, measured at 50 Hz frequency and room temperature. Compared to pure PVDF, the $FAPbI_3$ incorporated composites exhibit significantly enhanced ferroelectric behavior. Pure PVDF shows a weak P-E response, while the nanocomposites display higher polarization under applied electric fields. This improvement arises from the increased electroactive phase content in PVDF, which facilitates reorientation of ferroelectric domains, thereby enhancing the overall ferroelectric properties of the composites [7]. At any applied electric field, the energy storage density ($U_{stored}$) is evaluated by integrating the P-E hysteresis loop relative to the electric field axis, and the result is depicted in figure 2b. The results indicate that the FPF-3 composite showing the highest energy storage density value (215.27 mJ/cm$^3$) which is much higher than that of pure PVDF (89.43 mJ/cm$^3$). The increment in the energy storage density originates from the synergistic effects of increased electroactive phase content, enhanced interfacial polarization, and improved dielectric breakdown behavior arising from optimized polymer–filler interactions [8]. The piezoelectric properties, expressed in terms of remnant polarization ($P_r$) and maximum polarization ($P_{max}$), are shown in figure 2c. Remnant polarization, representing the residual lattice dipole moment after polarization, originates from heterogeneous polarization caused by charge accumulation at the interface between the $FAPbI_3$ and the PVDF matrix. In contrast, maximum polarization corresponds to the saturation polarization attained under the applied electric field [9]. The optimized composite has shown a maximum polarization of 0.03 μC/cm$^2$, whereas it is only 0.018 μC/cm$^2$ for the pure sample. On the other hand, the remnant polarization value for the optimized FPF-3 composite is 0.01 μC/cm$^2$, whereas it is only 0.001 μC/cm$^2$ for the pure sample. These findings highlight the potential of the composite film for advanced applications in piezoelectric energy harvesting and sensing.

Light-assisted energy harvesting using multifunctional perovskites has gained significant attention due to their ability

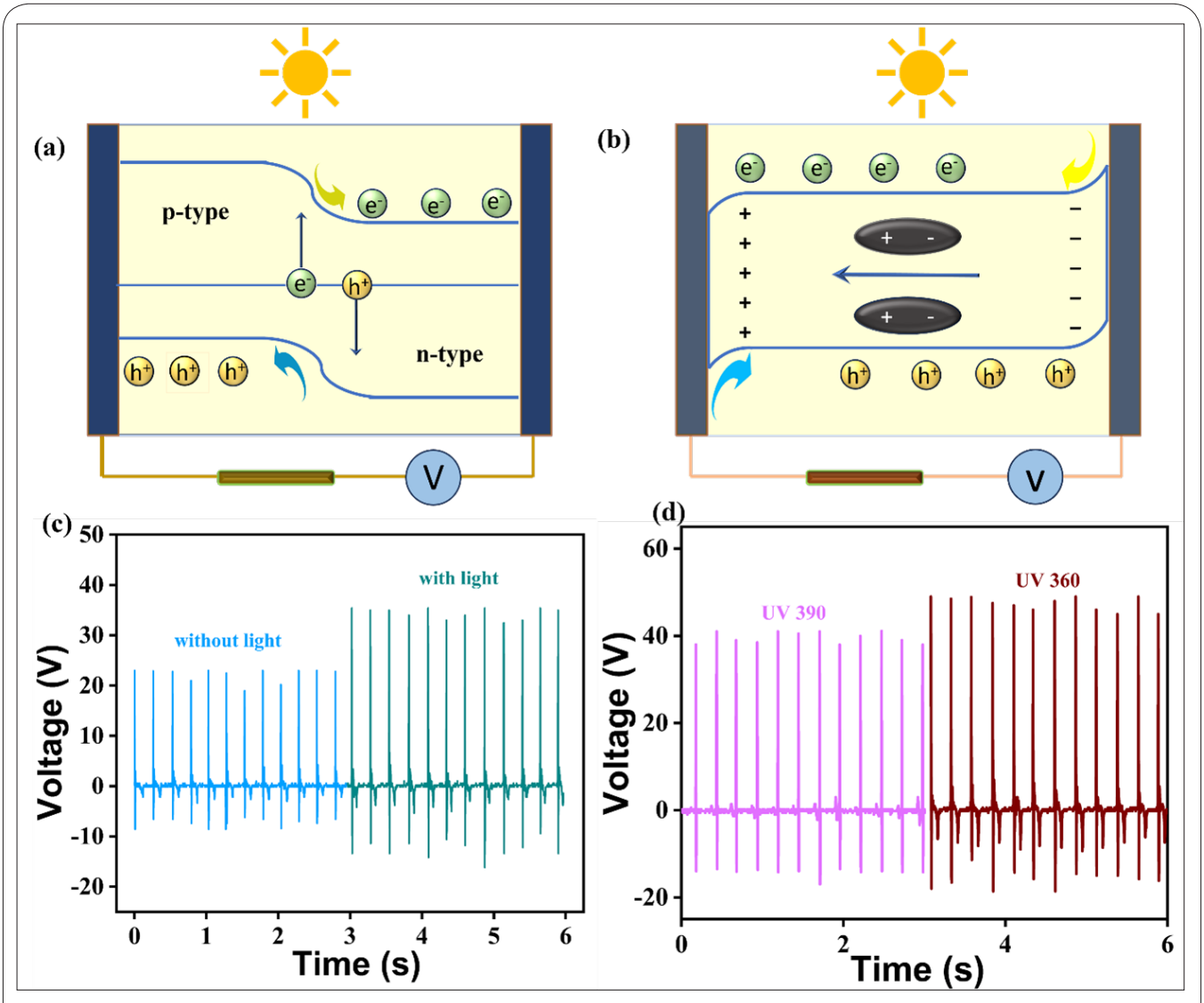



**Figure 3:** Light-assisted energy harvesting characteristics, **(a)** mechanism of exciton generation under photo-illumination, **(b)** piezo-photo synergistic charge separation process, **(c)** energy harvesting output under dark and illuminated conditions, and **(d)** performance comparison under UV-390 nm and UV-360 nm irradiation.

to generate excitons under illumination and exhibit excellent energy conversion properties. By coupling the photovoltaic effect with piezoelectric energy conversion of PVDF, the composites enabled enhanced charge density, stronger dipole moments, and reduced recombination losses under simultaneous mechanical and optical stimulation. The detailed mechanism related to that is depicted in figure 3a and figure 3b.

Among these, the black $\alpha^3$-phase of $FAPbI_3$ stands out for its superior photoactivity and photovoltaic efficiency. A flexible device fabricated out of optimized FPF-3 composite on ITO-coated PET and tested under hand tapping and different light conditions (represented in figure 3c and figure 3d) showed clear enhancement in output voltage, rising from ~23.7 V in dark to ~38.4 V under white light and further to ~62.6 V under 360 nm UV illumination and ~52.25 V under 390 nm UV, corresponding to a ~62.02% increase. These results highlight the strong potential of α-$FAPbI_3$/PVDF composites for efficient light-assisted energy harvesting applications.

## Conclusion

This work presents a simple and effective approach to stabilize the photoactive α-$FAPbI_3$ phase within a PVDF matrix, as verified by XRD analysis. Composite films with different $FAPbI_3$-PVDF ratios were systematically studied for their ferroelectric properties, including energy storage density, saturation polarization, and remnant polarization. Among them, the FPF-3 composition exhibited the best performance, with an energy storage density of 215.27 mJ/cm$^3$, saturation polarization of 0.03 μC/cm$^2$, and remnant polarization of 0.01 μC/cm$^2$. A light-assisted energy harvesting device fabricated from FPF-3 demonstrated distinct output responses under dark, white light, and UV illumination (360 and 390 nm), achieving ~62.02% higher output voltage under white light. These findings underscore its strong promise for next-generation photo-assisted, self-powered energy systems.

## Acknowledgements

The authors gratefully acknowledge financial support from the Industrial Research and Consultancy Center (IRCC), IIT Bombay, through the Faculty Seed Grant RD/0522-IRCCSH0-022, and from DST-SERB (CRG/2023/000183). The authors also thank the Department of Metallurgical Engineering and Materials Science, IIT Bombay, for providing characterization facilities.

## Conflict of Interest

None.

### References

1. Kojima A, Teshima K, Shirai Y, Miyasaka T. 2009. Organometal halide perovskites as visible-light sensitizers for photovoltaic cells. *J Am Chem Soc* 131(17): 6050-6051. https://doi.org/10.1021/ja809598r
2. Fabini DH, Stoumpos CC, Laurita G, Kaltzoglou A, Kontos AG, et al. 2016. Reentrant structural and optical properties and large positive thermal expansion in perovskite formamidinium lead iodide. *Angew Chem Int Ed Engl* 55(49): 15392-15396. https://doi.org/10.1002/anie.201609538
3. Nayak M, Nag R, Bera A, Samanta P, Akhtar AJ, et al. 2023. *In-situ* fabricated poly (vinylidene fluoride)-incorporated perovskite nanocrystals with better Schottky performance and enhanced stability. *Opt Mater* 138: 113685. https://doi.org/10.1016/j.optmat.2023.113685
4. Nayak M, Nag R, Bera A, Akhtar AJ, Saha SK. 2022. Schottky analysis of formamidinium lead halide perovskite nanocrystals' devices with enhanced stability. *Appl Nanosci* 12: 2671-2681. https://doi.org/10.1007/s13204-022-02535-1
5. Murugadoss G, Arunachalam P, Panda SK, Kumar MR, Rajabathar JR, et al. 2021. Crystal stabilization of α-$FAPbI_3$ perovskite by rapid annealing method in industrial scale. *J Mater Res Technol* 12: 1924-1930. https://doi.org/10.1016/j.jmrt.2021.03.107
6. Salim KMM, Masi S, Gualdrón-Reyes AF, Sánchez RS, Barea EM, et al. 2021. Boosting long-term stability of pure formamidinium perovskite solar cells by ambient air additive assisted fabrication. *ACS Energy Lett* 6(10): 3511-3521. https://doi.org/10.1021/acsenergylett.1c01311
7. Pratihar S, Chandran A, Bhat A, Mural PK. 2024. Piezoelectric nanogenerators based on poly(vinylidene fluoride) doped with high entropy oxide nanoparticles for sensitive pressure sensors. *ACS Appl Nano Mater* 7(17): 20553-20568. https://doi.org/10.1021/acsanm.4c03569
8. Cheng R, Wang Y, Men R, Lei Z, Song J, et al. 2022. High-energy-density polymer dielectrics via compositional and structural tailoring for electrical energy storage. *iScience* 25(8): 1-44. https://doi.org/10.1016/j.isci.2022.104837
9. Furukawa T, Date M, Fukada E. 1980. Hysteresis phenomena in polyvinylidene fluoride under high electric field. *J Appl Phys* 51(2): 1135-1141. https://doi.org/10.1063/1.327723